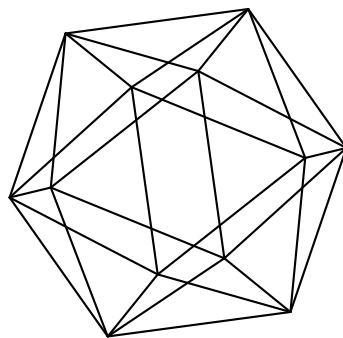


Max-Planck-Institut für Mathematik Bonn

Macdonald topological vertices and brane condensates

by

Omar Foda
Masahide Manabe



Macdonald topological vertices and brane condensates

Omar Foda
Masahide Manabe

Max-Planck-Institut für Mathematik
Vivatsgasse 7
53111 Bonn
Germany

Mathematics and Statistics
University of Melbourne
Royal Parade
Parkville VIC 3010
Australia

MACDONALD TOPOLOGICAL VERTICES AND BRANE CONDENSATES

OMAR FODA¹ AND MASAHIDE MANABE²

ABSTRACT. We show, in a number of simple examples, that Macdonald-type qt -deformations of topological string partition functions are equivalent to topological string partition functions that are without qt -deformations but with brane condensates, and that these brane condensates lead to geometric transitions.

1. INTRODUCTION

We recall the topological vertex, its refinements and deformations, and ask what the physical interpretation of a specific Macdonald-type deformation is.

1.1. A hierarchy of topological vertices.

1.1.1. *Abbreviations.* To simplify the presentation, we use **1.** *string, string partition function, vertex, etc.* for *topological string, topological string partition function, topological vertex, etc.*, which should cause no confusion, as we only consider the latter, and use *topological* only for emphasis when that is needed, **2.** *qt-string partition function, qt-quantum curve, etc.* for *qt-deformed string partition function, qt-deformed quantum curve, etc.* **3.** *refined* as in *refined partition functions, etc.*, when discussing objects that are refined in the sense of [9, 10, 32]; otherwise, no refinement should be inferred, and *unrefined* is used only for emphasis when that is needed, and finally, **4.** *the xy-version of \dots* for the version of an object that is refined in the sense of [9, 10, 32], and *the qt-version of \dots* for the version of an object that is deformed in the sense of [50, 18].

1.1.2. *The original vertex as a normalized 1-parameter generating function of plane partitions with fixed asymptotic boundaries.* In [2], Aganagic, Klemm, Mariño and Vafa introduced a systematic approach to compute A -model string partition functions using *the vertex* $C_{Y_1 Y_2 Y_3}(x)$, which we refer to as *the original vertex*.¹ It depends on a single parameter x , and a set of three Young diagrams, Y_1 , Y_2 and Y_3 , and has a combinatorial interpretation as a normalized partition function of 3D plane partitions [45], where each box in each plane partition is assigned a weight x . All plane partitions generated by $C_{Y_1 Y_2 Y_3}(x)$ satisfy fixed asymptotic boundary conditions specified by Y_1 , Y_2 and Y_3 . Copies of $C_{Y_1 Y_2 Y_3}(x)$ can be glued to form string partition functions. Using geometric engineering [35, 36], these string partition functions are identified with instanton partition functions in 5D supersymmetric gauge theories on $\mathbb{R}^4 \times S^1$, in a self-dual Ω -background with Nekrasov parameters $\epsilon_1 + \epsilon_2 = 0$ [40, 41]. Using the AGT/W correspondence [5, 51], the 4D limit of these 5D instanton partition functions are identified with conformal blocks in 2D conformal field theories with an integral central charge c .

Key words and phrases. Topological vertex. Brane condensation. Geometric transition. Topological string partition function. Quantum spectral curve.

¹ To streamline the presentation, we make a number of departures from conventional notation. We state these changes as we introduce them, and list them in section 2.1.1. In particular, we use x , instead of q , for the weight of a box in $C_{Y_1 Y_2 Y_3}(x)$.

1.1.3. *The refined vertex as a normalized 2-parameter generating function of plane partitions with fixed asymptotic boundaries.* In [9, 10], Awata and Kanno introduced a refined version of $C_{Y_1 Y_2 Y_3}(x)$, and in [32], Iqbal, Kozcaz and Vafa introduced yet another refined version of the same object. In [7], Awata, Feigin and Shiraishi proved that these two refinements are equivalent. In this work, we focus on *the refined vertex* $\mathcal{R}_{Y_1 Y_2 Y_3}(x, y)$ of [32].² It depends on two parameters (x, y) , and a set of three Young diagrams, Y_1 , Y_2 and Y_3 , and has a combinatorial interpretation as a normalized partition function of 3D plane partitions. Each box in each plane partition is assigned a weight x or y as follows. One splits each plane partition diagonally into vertical Young diagrams. Scanning the vertical Young diagrams from one end to the other, a box in a plane partition is assigned a weight x if it belongs to a vertical Young diagram that protrude with respect to the preceding Young diagram, and a weight y if it belongs to a vertical Young diagram that does not. All plane partitions generated by $\mathcal{R}_{Y_1 Y_2 Y_3}(x, y)$ satisfy fixed asymptotic boundary conditions specified by Y_1 , Y_2 and Y_3 . Copies of $\mathcal{R}_{Y_1 Y_2 Y_3}(x, y)$ can be glued to form refined string partition functions. Using geometric engineering [35, 36], these refined string partition functions are identified with instanton partition functions in 5D supersymmetric gauge theories on $\mathbb{R}^4 \times S^1$, in a generic Ω -background, with Nekrasov parameters $\epsilon_1 + \epsilon_2 \neq 0$ [40, 41]. Using the AGT/W correspondence [5, 51], the 4D limits of these 5D instanton partition functions are identified with conformal blocks in 2D conformal field theories with a non-integral central charge c .

1.1.4. *The Macdonald vertex as a qt -deformation of the refined vertex.* In [50], Vuletić introduced a deformation of MacMahon's generating function of plane partitions, in terms of two Macdonald-type parameters (q, t) . This deformation is independent of the refinement introduced in [9, 10] and [32], as one can check by considering $\mathcal{R}'_{\emptyset \emptyset \emptyset}(x, y)$, the unnormalized version of $\mathcal{R}_{\emptyset \emptyset \emptyset}(x, y)$, which is a refinement of MacMahon's generating function, but is different from that of [50]. In [18], $\mathcal{R}_{Y_1 Y_2 Y_3}(x, y)$ was deformed using the same Macdonald-type parameters (q, t) that were used in [50], to obtain *the Macdonald vertex* $\mathcal{M}_{Y_1 Y_2 Y_3}^{qt}(x, y)$.³ Copies of $\mathcal{M}_{Y_1 Y_2 Y_3}^{qt}(x, y)$ can be glued to form qt -string partition functions that are 5D qt -instanton partition functions. The latter have well-defined 4D-limits and, for generic values of (q, t) , contain infinite-towers of poles for every pole that is present in the limit $q \rightarrow t$ [18].

1.1.5. *Limits of the Macdonald vertex.* In constructing the original and the refined vertex, (undeformed) free bosons that satisfy the Heisenberg algebra,

$$(1.1) \quad [a_m, a_n] = n \delta_{m+n, 0},$$

play a central role [45, 32]. Similarly, in constructing the Macdonald vertex, qt -free bosons that satisfy the qt -Heisenberg algebra,

$$(1.2) \quad [a_m^{qt}, a_n^{qt}] = n \left(\frac{1 - q^{|n|}}{1 - t^{|n|}} \right) \delta_{m+n, 0},$$

² We use (x, y) instead of (q, t) for the parameters, and $\mathcal{R}_{Y_1 Y_2 Y_3}(x, y)$ instead of $C_{Y_1 Y_2 Y_3}(t, q)$ for the refined vertex of [32]. We reserve the parameters (q, t) for the Macdonald-type deformation parameters of [50, 18] introduced in section 1.1.4.

³ We call the ratio x/y a *refinement*, and in the limit $x \rightarrow y$, the refined vertex reduces to the original one, and we call the ratio q/t a *deformation*, and in the limit $q \rightarrow t$, the Macdonald vertex reduces to the original vertex, for $x = y$, or to the refined vertex, for $x \neq y$.

play a central role. In the limit $q \rightarrow t$, $\mathcal{M}_{Y_1 Y_2 Y_3}^{qt}(x, y) \rightarrow \mathcal{R}_{Y_1 Y_2 Y_3}(x, y)$, and in the limit $x \rightarrow y$, $\mathcal{M}_{Y_1 Y_2 Y_3}^{qt}(x, y) \rightarrow \mathcal{C}_{Y_1 Y_2 Y_3}^{qt}(x)$, which is a qt -deformation of $\mathcal{C}_{Y_1 Y_2 Y_3}(x)$.

1.2. The physical interpretation of the qt -deformation. It is clear by inspection of explicit computations that the Macdonald parameter ratio q/t is a different object from either the M -theory circle radius R or the refinement parameter ratio x/y .⁴ The purpose of this work is to shed light on the geometric and/or physical interpretation of the qt -deformation. To do this, we consider simple string partition functions, and show that in M -theory terms, the deformation $q/t \neq 1$ describes a condensation of $M5$ -branes that lead to geometric transitions that change the topology of the original Calabi-Yau 3-fold [23]. In conformal field theory terms, we expect that it describes a condensation of vertex operators that push the conformal field theory off criticality [52].

1.3. Outline of contents. In section 2, we include comments on notation used in the text, and definitions of combinatorial objects, including MacMahon's generating function of plane partitions, its refinement and qt -deformation, and in 3, include basic facts related to the original topological vertex, the refined topological vertex, and their qt -deformations. In section 4, we give our first example of the equivalence of qt -deformation and brane condensation, which shows that the refined qt -string partition function on \mathbb{C}^3 is equivalent to a refined string partition function on \mathbb{C}^3 with no qt -deformation but in the presence of brane condensates, and in 5, we give our second example, which shows that a refined qt -deformed partition function on \mathbb{C}^3 with a single-brane insertion is equivalent to its counterpart (also with a single-brane insertion) with no qt -deformation but in the presence of brane condensates. In section 6, we discuss the relation of brane condensates and geometric transitions in the context of unrefined objects, and in 7, we discuss the qt -quantum curves associated with qt -partition function. Finally, in section 8, we collect a number of remarks, and discuss the various parameters that can appear in topological vertices and the relation with conformal field theory, and in appendix A, we collect useful skew Schur function identities that are used freely in the text.

2. NOTATION AND DEFINITIONS

We collect comments on notation, definitions of combinatorial objects, including variations on MacMahon's generating function of plane partitions that appear in the sequel.

2.1. Notation.

2.1.1. Deviations from standard notation. We use the variables (x, y) as box weights/refinement parameters, instead of the variables (q, t) used in [9, 10, 32]. We use $\mathcal{R}_{Y_1 Y_2 Y_3}(x, y)$ for the refined vertex instead of $\mathcal{C}_{Y_1 Y_2 Y_3}(t, q)$ as used in [32].⁵ We reserve the variables (q, t) for the Macdonald-type deformation parameters that appear in the Macdonald vertex $\mathcal{M}_{Y_1 Y_2 Y_3}^{qt}(x, y)$ of [18].

2.1.2. Sets. ρ is the set of negative half-integers (ρ_1, ρ_2, \dots) with $\rho_i = -i + 1/2$, that is $(\rho_1, \rho_2, \dots) = (-1/2, -3/2, \dots)$, and ι is the set of non-zero positive integers $(1, 2, \dots)$.

2.2. Combinatorics.

⁴ One can also introduce an elliptic nome p [29, 33, 53, 19], which is yet another parameter. In section 8.2, we discuss what we know about the interpretation of the for parameters, R , x/y , q/t , and p .

⁵ See section 3.2.2 for a more detailed relation.

2.2.1. *Cells in the lower-right quadrant.* Consider the lower-right quadrant in \mathbb{R}^2 , bounded by the right-half of the x -axis and the lower-half of the y -axis. The intersection point of the x - and y -axes to be the origin with coordinates $(0,0)$, the x -coordinate increases to the right, the y -coordinate increases downwards. We divide this quadrant into cells of unit-length in each direction. A cell \square has coordinates (i, j) , if the coordinates of the lower-right corner of the cell are (i, j) .

2.2.2. *Young diagrams.* Y is a Young diagram in the lower-right quadrant of \mathbb{R}^2 that consists of rows of cells of positive integral lengths $y_1 \geq y_2 \geq \dots \geq 0$, and Y' is the transpose of Y that consists of rows of cells of positive integral lengths $y'_1 \geq y'_2 \geq \dots \geq 0$. y'_1 is the number of (non-zero) parts in Y . The infinite profile of Y consists of the union of **1.** a semi-infinite line that extends from right to left along the positive, right-half of the x -axis, from $x = \infty$ to $x = y_1$, **2.** the finite profile of Y , and **3.** a semi-infinite line that extends from top to bottom along the positive, lower-half of the y -axis, from $y = y'_1$ to $y = \infty$.⁶

2.2.3. *Arms, legs and hook lengths.* Consider a Young diagram Y , and a cell \square_{ij} with coordinates (i, j) such that \square_{ij} is *not* necessarily inside Y . The arm $A_{\square_{ij}}$, leg $L_{\square_{ij}}$, extended arm $A_{\square_{ij}}^+$, extended leg $L_{\square_{ij}}^+$, and hook $H_{\square_{ij}}$ of \square_{ij} , with respect to the infinitely-extended profile of Y , are,

$$(2.1) \quad A_{\square_{ij}} = y_i - j, \quad L_{\square_{ij}} = y'_j - i, \quad A_{\square_{ij}}^+ = A_{\square_{ij}} + 1, \quad L_{\square_{ij}}^+ = L_{\square_{ij}} + 1, \quad H_{\square_{ij}} = A_{\square_{ij}} + L_{\square_{ij}} + 1,$$

where y'_j is the length of the j -row in Y' , which is the j -column in Y . We also define,

$$(2.2) \quad |Y| = \sum_{\square \in Y} 1, \quad \frac{1}{2} \|Y\|^2 = \sum_{\square \in Y} \left(A_{\square} + \frac{1}{2} \right), \quad \frac{1}{2} \kappa_Y = \frac{1}{2} (\|Y\|^2 - \|Y'\|^2) = \sum_{(i,j) \in Y} (j - i)$$

2.3. **The framing factor.** We use the notation $f_Y(x)$ for the framing factor of the original vertex [39, 2],

$$(2.3) \quad f_Y(x) = (-1)^{|Y|} x^{\frac{1}{2} \kappa_Y},$$

and,

$$(2.4) \quad f_Y(x, y) = (-1)^{|Y|} x^{-\frac{1}{2} \|Y'\|^2} y^{\frac{1}{2} \|Y\|^2},$$

for the refined framing factor introduced in [48] of the refined vertex.

2.4. **Splitting indices.** Starting from a sequence $\mathbf{a} = (a_1, a_2, \dots)$, one can split the single index I of any element a_I into two indices ij , so that $a_I \rightarrow a_{ij}$. One way to split the indices is in the following example.

⁶ In our notation, the positive half of y -axis is the lower-half that extends downwards.

2.4.1. *Example.* We proceed in two steps. 1. Position the elements of the 1-dimensional sequence (a_1, a_2, \dots) along the anti-diagonals of a 2-dimensional array, as in,

$$(2.5) \quad (a_1, a_2, \dots) \mapsto \begin{array}{cccc} a_1 & a_2 & a_4 & \cdots \\ & a_3 & a_5 & \\ & & a_6 & \end{array}$$

2. Map the array with single-index elements to an array with double-index elements, where the double-indices are in conventional order, as in,

$$(2.6) \quad \begin{array}{cccc} a_1 & a_2 & a_4 & \cdots \\ a_3 & a_5 & & \\ a_6 & & & \end{array} \mapsto \begin{array}{cccc} a_{11} & a_{12} & a_{13} & \cdots \\ a_{21} & a_{22} & & \\ a_{31} & & & \end{array}$$

Any such splitting of indices is far from unique. However, if the splitting rule is well-defined, as in (2.5)–(2.6), then it is bijective, and all such splittings are in bijection *via* the original 1-dimensional sequence.

2.5. Variations on MacMahon's generating functions.

2.5.1. *Notation.* To streamline the notation, we use the redundant notation M_{xx} for MacMahon's original generating function of plane partitions, so that we can write M_{xy} for its refined counterpart, and M_{xy}^{qt} for the qt -version of the latter. M_{xx}^{qt} is the qt -MacMahon generating function of Vuletić, and $M_{xy}^{qq} = M_{xy}$.

2.5.2. M_{xx} . MacMahon's generating function of plane partitions is,

$$(2.7) \quad M_{xx} = \prod_{m=1}^{\infty} \left(\frac{1}{1-x^m} \right)^m = \exp \left(\sum_{n=1}^{\infty} \frac{1}{n (x^{n/2} - x^{-n/2})^2} \right)$$

The first equation in (2.7) is the definition of the MacMahon generating function. The second is obtain by direct expansion of the logarithms of both sides. All xy - and qt -versions of this equation, in the sequel, are proven similarly.

2.5.3. M_{xy} . The xy -version MacMahon's generating function of plane partitions is [32],

$$(2.8) \quad M_{xy} = \prod_{m,n=1}^{\infty} \frac{1}{1-x^m y^{n-1}} = \exp \left(\sum_{n=1}^{\infty} \frac{(x/y)^{n/2}}{n (x^{n/2} - x^{-n/2}) (y^{n/2} - y^{-n/2})} \right)$$

In the limit $y \rightarrow x$, $M_{xy} \rightarrow M_{xx}$.

2.5.4. M_{xx}^{qt} . The qt -version MacMahon's generating function of plane partitions is,

$$(2.9) \quad M_{xx}^{qt} = \prod_{i=0}^{\infty} \prod_{m=1}^{\infty} \left(\frac{1 - q^i t x^m}{1 - q^i x^m} \right)^m = \exp \left(\sum_{n=1}^{\infty} \frac{1}{n (x^{n/2} - x^{-n/2})^2} \left(\frac{1 - t^n}{1 - q^n} \right) \right)$$

which is the qt -MacMahon generating function introduced by Vuletić in [50]. In the limit $t \rightarrow q$, $M_{xx}^{qt} \rightarrow M_{xx}^{qq} = M_{xx}$.

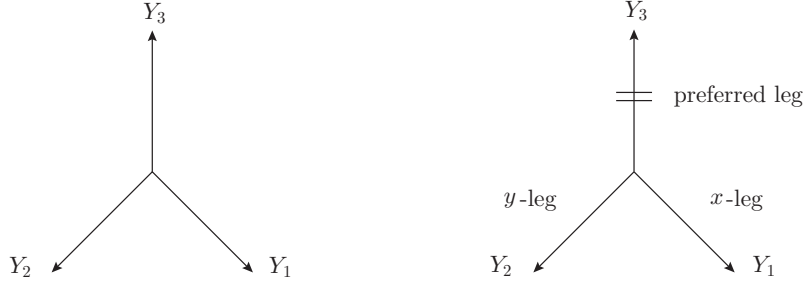


FIGURE 3.1. The figure on the left represents the vertex $C_{Y_1 Y_2 Y_3}(x)$, and this vertex has the cyclic symmetry $C_{Y_1 Y_2 Y_3}(x) = C_{Y_3 Y_1 Y_2}(x) = C_{Y_2 Y_3 Y_1}(x)$. The figure on the right represents the refined vertex $\mathcal{R}_{Y_1 Y_2 Y_3}(x, y)$ and the Macdonald vertex $M_{Y_1 Y_2 Y_3}^{qt}(x, y)$. These two vertices break the cyclic symmetry and have the preferred leg. Note that $\mathcal{R}_{Y_1 Y_2 Y_3}(x, x) = C_{Y_1 Y_2 Y_3'}(x)$.

2.5.5. M_{xy}^{qt} . The xy -refined and qt -deformed version MacMahon's generating function of plane partitions is [18],

$$(2.10) \quad M_{xy}^{qt} = \prod_{i=0}^{\infty} \prod_{m,n=1}^{\infty} \frac{1 - q^i t x^m y^{n-1}}{1 - q^i x^m y^{n-1}} = \exp \left(\sum_{n=1}^{\infty} \frac{(x/y)^{n/2}}{n (x^{n/2} - x^{-n/2}) (y^{n/2} - y^{-n/2})} \left(\frac{1 - t^n}{1 - q^n} \right) \right)$$

In the limit $y \rightarrow x$, $M_{xy}^{qt} = M_{xx}^{qt}$, and so on.

3. TOPOLOGICAL VERTICES

We recall basic facts related to the topological vertices introduced in section 1.1.

3.1. **The original vertex of [2].** With reference to the figure on the left in Fig. 3.1, the normalized version of the original vertex⁷ of [2] is,

$$(3.1) \quad C_{Y_1 Y_2 Y_3}(x) = x^{\frac{1}{2} \kappa_{Y_1}} s_{Y_3}(x^\rho) \sum_Y s_{Y_1/Y}(x^{\rho+Y_3}) s_{Y_2/Y}(x^{\rho+Y_3}) \\ = (-1)^{|Y_2|+|Y_3|} f_{Y_1}(x) x^{\frac{1}{2} \|Y_3\|^2} \left(\prod_{\square \in Y_3} \frac{1}{1 - x^{H_\square}} \right) \sum_Y s_{Y_1/Y}(x^{-\rho-Y_3}) s_{Y_2/Y}(x^{-\rho-Y_3})$$

Here $x^{\rho+Y} = (x^{\rho_1+y_1}, x^{\rho_2+y_2}, \dots)$, $x = e^{-g_s}$, where g_s is the string coupling constant, and $s_{Y_1/Y_2}(x)$ is the skew Schur function defined in terms of a pair of Young diagrams (Y_1, Y_2) and a set of possibly infinitely-many variables $\mathbf{x} = (x_1, x_2, \dots)$. In the second equality, we have used the notation $f_Y(x)$ for the framing factor (2.3), and the identities in appendix A.

3.1.1. *Normalization.* $C_{Y_1 Y_2 Y_3}(x)$ is normalized by M_{xx} such that $C_{\emptyset \emptyset \emptyset}(x) = 1$. The unnormalized version is,

$$(3.2) \quad C'_{Y_1 Y_2 Y_3}(x) = M_{xx} C_{Y_1 Y_2 Y_3}(x)$$

⁷ In the present work, we use x for the weight of a box in a plane partition, instead of q in [2]. For a review of the original vertex, see [38].

3.1.2. $C'_{Y_1 Y_2 Y_3}(x)$ and M_{xx} as partition functions. $C'_{Y_1 Y_2 Y_3}(x)$ is the open topological A -model partition function on \mathbb{C}^3 with three special Lagrangian submanifolds. M_{xx} is the closed topological A -model partition function on \mathbb{C}^3 . The figure on the left in Fig. 3.1 is the toric web diagram of \mathbb{C}^3 .

3.1.3. *Choice of framing.* One can choose the framing of $C_{Y_1 Y_2 Y_3}(x)$ as,

$$(3.3) \quad C_{Y_1 Y_2 Y_3}(x) \rightarrow \left(\prod_{i=1,2,3} f_{Y_i}(x)^{f_i} \right) C_{Y_1 Y_2 Y_3}(x), \quad f_1, f_2, f_3 \in \mathbb{Z},$$

where $f_Y(x)$ is the framing factor (2.3).

3.2. **The refined vertex of [32].** With reference to the figure on the right in Fig. 3.1, the normalized refined vertex of [32] is,

$$(3.4) \quad \mathcal{R}_{Y_1 Y_2 Y_3}(x, y) = (-1)^{|Y_2|+|Y_3|} f_{Y_1}(x, y) x^{\frac{1}{2}\|Y'_3\|^2} \left(\prod_{\square \in Y_3} \frac{1}{1 - x^{L_{\square}^+} y^{A_{\square}}} \right) \times \\ \sum_Y \left(\frac{y}{x} \right)^{\frac{1}{2}(|Y|-|Y_1|+|Y_2|)} s_{Y_1/Y}(y^{-\rho} x^{-Y'_3}) s_{Y'_2/Y}(x^{-\rho} y^{-Y_3}),$$

where $f_Y(x, y)$ is the refined framing factor (2.4). In the limit $y \rightarrow x$,

$$(3.5) \quad \mathcal{R}_{Y_1 Y_2 Y_3}(x, y) \rightarrow C_{Y_1 Y_2 Y'_3}(x)$$

3.2.1. *Remark.* The dependence on the Young diagram Y_3 in $\mathcal{R}_{Y_1 Y_2 Y_3}(x, y)$ on the left hand side of (3.5) is replaced by a dependence on its transpose Y'_3 in $C_{Y_1 Y_2 Y'_3}(x)$ on the right hand side.

3.2.2. *Remark.* (t, q) in [32] become (x, y) in the present work, and the refined vertex $C_{Y_1 Y_2 Y_3}(t, q)$ in [32] is related to $\mathcal{R}_{Y_1 Y_2 Y_3}(x, y)$ in the present work by,

$$(3.6) \quad C_{Y_1 Y_2 Y_3}(t, q) = (-1)^{|Y_1|+|Y_2|} f_{Y_3}(x, y) \mathcal{R}_{Y_2 Y_1 Y_3}(x, y)$$

3.2.3. *Choice of framing.* One can choose the framing of $\mathcal{R}_{Y_1 Y_2 Y_3}(x, y)$ as,

$$(3.7) \quad \mathcal{R}_{Y_1 Y_2 Y_3}(x, y) \rightarrow \left(\prod_{i=1,2,3} f_{Y_i}(x, y)^{f_i} \right) \mathcal{R}_{Y_1 Y_2 Y_3}(x, y), \quad f_1, f_2, f_3 \in \mathbb{Z}$$

3.2.4. *Normalization.* $\mathcal{R}_{Y_1 Y_2 Y_3}(x, y)$ is normalized by M_{xy} such that $\mathcal{R}_{\emptyset \emptyset \emptyset}(x) = 1$. The unnormalized version is,

$$(3.8) \quad \mathcal{R}'_{Y_1 Y_2 Y_3}(x, y) = M_{xy} \mathcal{R}_{Y_1 Y_2 Y_3}(x, y)$$

3.3. The Macdonald vertex of [18]. With reference to the figure on the right in Fig. 3.1, the normalized Macdonald vertex of [18] is,

$$(3.9) \quad \mathcal{M}_{Y_1 Y_2 Y_3}^{qt}(x, y) = \left(\prod_{i=0}^{\infty} \prod_{\square \in Y_3} \frac{1 - q^i t x^{L_{\square}^+} y^{A_{\square}}}{1 - q^i x^{L_{\square}^+} y^{A_{\square}}} \right) \sum_Y P_{Y_1/Y}^{qt}(y^{t-1} x^{-Y'_3}) Q_{Y_2/Y}^{qt}(x^t y^{-Y_3})$$

Here $P_{Y_1/Y_2}^{qt}(\mathbf{x})$ and $Q_{Y_1/Y_2}^{qt}(\mathbf{x})$ are the skew Macdonald and dual Macdonald functions defined for a pair of Young diagrams (Y_1, Y_2) and a set of possibly infinitely-many variables $\mathbf{x} = (x_1, x_2, \dots)$.

3.3.1. Choice of framing. No choice of framing of $\mathcal{M}_{Y_1 Y_2 Y_3}^{qt}(x, y)$ was discussed in [18], and none will be needed in the present work.

3.3.2. Normalization. $\mathcal{M}_{Y_1 Y_2 Y_3}^{qt}(x, y)$ is normalized by M_{xx}^{qt} such that $\mathcal{M}_{\emptyset \emptyset \emptyset}^{qt}(x, y) = 1$. The unnormalized version is,

$$(3.10) \quad \mathcal{M}'_{Y_1 Y_2 Y_3}{}^{qt}(x, y) = M_{xy}^{qt} \mathcal{M}_{Y_1 Y_2 Y_3}^{qt}(x, y)$$

4. A qt -PARTITION FUNCTION FROM BRANE CONDENSATES

We give an example of a refined qt -deformed partition function that is obtained from its undeformed counterpart via brane condensation.

4.1. From M5-branes to surface operators. Consider M-theory on,

$$(4.1) \quad \mathbb{R}^4 \times S^1 \times X,$$

where S^1 is the M-theory circle, and X is a local toric Calabi-Yau 3-fold such that the topological A-model on X geometrically engineers a 5D $SU(N)$ supersymmetric gauge theory on $\mathbb{R}^4 \times S^1$ with $(\mathbb{C}^\times)^2$ -equivariant parameters x, y acting on \mathbb{R}^4 (Ω -background) [35, 36]. We introduce M5-branes on the submanifold,

$$(4.2) \quad \mathbb{R}^2 \times S^1 \times L \subset \mathbb{R}^4 \times S^1 \times X,$$

where $L \cong S^1 \times \mathbb{C}$ is a Lagrangian submanifold in X [28] such that an end-point of L is on an edge of the toric web diagram [3]. The M5-branes geometrically engineer simple-type half-BPS surface operators that reduce the gauge group to $SU(N-1) \times U(1)$ on the surface \mathbb{R}^2 [26, 6, 13, 34].

4.2. From surface operators to primary-field vertex operators. The AGT/W correspondence [5, 51] relates a class of 4D $\mathcal{N} = 2$ supersymmetric gauge theories on \mathbb{R}^4 to 2D Toda conformal field theories. Each of these Toda conformal field theories is defined on a punctured Riemann surface that is related to the Seiberg-Witten curve of the gauge theory and to the mirror curve of the Calabi-Yau 3-fold X . The simple-type surface operators on the gauge theory side correspond to vertex operators that, in turn, correspond to the highest-weight states in irreducible fully-degenerate highest-weight representations on the conformal field theory side [4, 17]. In other words, the M5-branes in (4.2) correspond to primary-field vertex operators of fully-degenerate representations in Toda conformal field theory [37, 17, 49, 8]. From that it follows that a condensation of the M5-branes corresponds to a condensation of

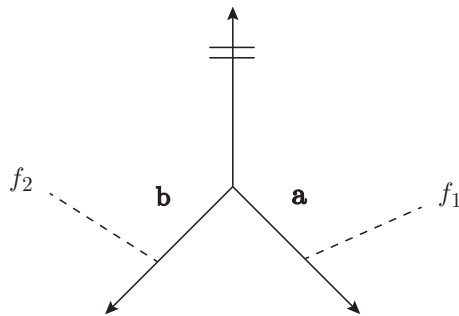


FIGURE 4.1. The vertex with two infinite stacks of branes with open string moduli $\mathbf{a} = (a_I)_{I=1,2,\dots}$, $\mathbf{b} = (b_I)_{I=1,2,\dots}$ and framing factors f_1 and f_2 .

vertex operators. We expect that such a condensation leads to an off-critical deformation of the chiral blocks in the conformal field theory of the type that leads to correlation functions in off-critical integrable models. We will say more about this in section 8. In the following we show that for $X = \mathbb{C}^3$, condensates of M5-branes lead to the qt -MacMahon generating function (2.9).

4.3. A qt -partition function from two brane condensates.

4.3.1. *The normalized version of the computation.* Starting from the refined open string partition function on \mathbb{C}^3 , which is the refined vertex, we trivialize the Young diagram on one of the three legs, and add a stack of infinitely-many branes on each of the two other legs. The first stack has open string moduli $\mathbf{a} = (a_1, a_2, \dots)$, and framing factor f_1 , and the second has $\mathbf{b} = (b_1, b_2, \dots)$, and framing factor f_2 , as indicated in Fig. 4.1. The result is the open string partition function⁸,

$$(4.3) \quad Z_{xy}^{(f_1, f_2)}(\mathbf{a}, \mathbf{b}) = \mathcal{N}_{branes} \sum_{Y_1, Y_2} \left(\prod_{i=1,2} f_{Y_i}^{f_i}(x, y) \right) \mathcal{R}_{Y_1 Y_2 \emptyset}(x, y) s_{Y_1}(\mathbf{a}) s_{Y_2}(\mathbf{b}),$$

where \mathcal{N}_{branes} is a normalization factor, due to the introduction of the branes to be determined in the sequel. Choosing $(f_1, f_2) = (-1, 0)$ we get

$$(4.4) \quad Z_{xy}^{(-1, 0)}(\mathbf{a}, \mathbf{b}) = \mathcal{N}_{branes} \sum_{Y_1, Y_2, Y} v^{-|Y|} s_{Y_1/Y}(y^{-\rho}) s_{Y_1}(v\mathbf{a}) s_{Y_2/Y}(x^{-\rho}) s_{Y_2}(-v^{-1}\mathbf{b}),$$

where $v = x^{1/2}/y^{1/2}$. Using the Cauchy identities in appendix A we obtain

$$(4.5) \quad Z_{xy}^{(-1, 0)}(\mathbf{a}, \mathbf{b}) = \mathcal{N}_{branes} \left(\prod_{I,J=1}^{\infty} (1 - v^{-1} a_I b_J) \right) \left(\prod_{I=1}^{\infty} \frac{L(v^{-1} b_I, x)}{L(v a_I, y)} \right),$$

where $L(a, x)$ is the quantum dilogarithm,

$$(4.6) \quad L(a, x) = \prod_{m=1}^{\infty} (1 - a x^{m-\frac{1}{2}}) = \exp \left(\sum_{n=1}^{\infty} \frac{a^n}{n (x^{n/2} - x^{-n/2})} \right)$$

⁸ In the absence of the condensates, we have a closed string partition function on \mathbb{C}^3 . The M5-branes that condense are equivalent to open strings.

To determine \mathcal{N}_{branes} , we normalize $Z_{xy}^{(-1,0)}(\mathbf{a}, \mathbf{b})$ such that,

$$(4.7) \quad \lim_{x \rightarrow 0} Z_{xx}^{(-1,0)}(\mathbf{a}, \mathbf{b}) = 1,$$

so we take,

$$(4.8) \quad \mathcal{N}_{branes} = \prod_{I,J=1}^{\infty} \frac{1}{(1 - v^{-1}a_I b_J)},$$

and obtain,

$$(4.9) \quad Z_{xy}^{(-1,0)}(\mathbf{a}, \mathbf{b}) = \prod_{I=1}^{\infty} \frac{L(v^{-1}b_I, x)}{L(va_I, y)}, \quad v = \left(\frac{x}{y}\right)^{1/2}$$

The introduction of the normalization factor fixed by (4.8) means that we subtract the contribution of the brane-brane interactions between the two infinite stacks of branes, and only consider the individual brane condensates at each leg.

4.3.2. *The unnormalized version of the computation.* The above calculation started from the normalized vertex $\mathcal{R}_{Y_1 Y_2 Y_3}(x, y)$. If we use the unnormalized vertex $\mathcal{R}'_{Y_1 Y_2 Y_3}(x, y)$ in (3.8), we get the unnormalized brane partition function with two condensates,

$$(4.10) \quad Z'_{xy}^{(-1,0)}(\mathbf{a}, \mathbf{b}) = M_{xy} \prod_{I=1}^{\infty} \frac{L(v^{-1}b_I, x)}{L(va_I, y)}$$

Splitting the index $I \rightarrow (i, j)$, as in section 2.4, and setting,

$$(4.11) \quad a_I \rightarrow a_{ij} = q^i x^{j-\frac{1}{2}}, \quad b_I \rightarrow b_{ij} = q^{i-1} t x y^{j-\frac{3}{2}}, \quad i, j = 1, 2, \dots,$$

we find,

$$(4.12) \quad Z'_{xy}^{(-1,0)}(a_{ij}, b_{ij}) = M_{xy} \prod_{i,j=1}^{\infty} \frac{L(v^{-1}b_{ij}, x)}{L(va_{ij}, y)} = \prod_{i=0}^{\infty} \prod_{m,n=1}^{\infty} \frac{1 - q^i t x^m y^{n-1}}{1 - q^i x^m y^{n-1}} = M_{xy}^{qt}$$

Then we conclude that the refined open string partition function on \mathbb{C}^3 with the two infinite stacks of branes, with the moduli (4.11), agrees with the xy -refined qt -MacMahon generating function M_{xy}^{qt} in (2.10) which gives the refined qt -deformed closed string partition function on \mathbb{C}^3 .

By taking the unrefined limit $y \rightarrow x$ in (4.12), we also obtain,

$$(4.13) \quad Z'_{xx}^{(-1,0)}(a_{ij}, b_{ij}) = M_{xx} \prod_{i,j=1}^{\infty} \frac{L(b_{ij}, x)}{L(a_{ij}, x)} = \prod_{i=0}^{\infty} \prod_{m=1}^{\infty} \left(\frac{1 - q^i t x^m}{1 - q^i x^m} \right)^m = M_{xx}^{qt}$$

where the right hand side is Vuletić's qt -MacMahon generating function in (2.9) [50], and the left hand side can be derived using the original vertex $C_{Y_1 Y_2 Y_3}(x)$ as in [27].

4.3.3. *Remark.* The relations (4.12) and (4.13) agree with the result that conformal blocks computed using $\mathcal{M}_{Y_1 Y_2 Y_3}^{qt}(x, y)$ are equal to those computed using $\mathcal{R}_{Y_1 Y_2 Y_3}(x, y)$ up to a qt -dependent factor [18].

5. A qt -PARTITION FUNCTION WITH A SINGLE-BRANE INSERTION FROM BRANE CONDENSATES

We give an example of a refined qt -deformed partition function with a single-brane insertion that is obtained from its undeformed counterpart via brane condensation.

5.1. A partition function with two brane condensates and a single brane. Consider the same partition function as in section 4.3, but now with an additional brane (on the preferred leg of the refined vertex that has no stacks of branes) with open string modulus U and a framing factor f_3 , and two infinite stacks of branes (see Fig. 5.1),

$$(5.1) \quad Z_{xy}^{(f_1, f_2, f_3)}(U; \mathbf{a}, \mathbf{b}) = \mathcal{N}_{branes} \sum_{Y_1, Y_2, Y_3} \left(\prod_{i=1,2,3} f_{Y_i}(x, y)^{f_i} \right) \mathcal{R}_{Y_1 Y_2 Y_3}(x, y) s_{Y_1}(\mathbf{a}) s_{Y_2}(\mathbf{b}) s_{Y_3}(U)$$

Here \mathcal{N}_{branes} is the normalization factor introduced in (4.3) and determined in (4.8), and the Schur function $s_{Y_3}(U)$ with a single variable U is non-zero only for Young diagrams with a single row $y_1 = d$. Choosing the framing factors as $(f_1, f_2, f_3) = (-1, 0, f)$, we get,

$$(5.2) \quad Z_{xy}^{(-1, 0, f)}(U; \mathbf{a}, \mathbf{b}) = \mathcal{N}_{branes} \sum_{Y_1, Y_2, Y_3, Y} f_{Y_3'}(x, y)^f x^{\frac{1}{2}\|Y_3\|^2} \left(\prod_{\square \in Y_3} \frac{1}{1 - x^{A_{\square}^+} y^{L_{\square}}} \right) s_{Y_3}(-U) \times v^{-|Y_1|} s_{Y_1/Y}(y^{-\rho} x^{-Y_3}) s_{Y_1}(v\mathbf{a}) s_{Y_2'/Y}(x^{-\rho} y^{-Y_3'}) s_{Y_2}(-v^{-1}\mathbf{b}),$$

where $v = (x/y)^{1/2}$. Using the Cauchy identities in appendix A, we obtain,

$$(5.3) \quad Z_{xy}^{(-1, 0, f)}(U; \mathbf{a}, \mathbf{b}) = \mathcal{N}_{branes} \left(\prod_{I, J=1}^{\infty} (1 - v^{-1} a_I b_J) \right) \left(\prod_{I=1}^{\infty} \frac{L(v^{-1} b_I, x)}{L(va_I, y)} \right) \times \sum_{d=0}^{\infty} \frac{x^{\frac{1}{2}(1-f)d^2} \left((-1)^{f+1} y^{f/2} U \right)^d}{\prod_{m=1}^d (1 - x^m)} \left(\prod_{I=1}^{\infty} \frac{(1 - a_I x^{\frac{1}{2}})}{(1 - a_I x^{\frac{1}{2}-d})} \prod_{m=1}^d \frac{(1 - b_I x^{m-1} y^{-\frac{1}{2}})}{(1 - b_I x^{m-1} y^{\frac{1}{2}})} \right),$$

where $L(a, x)$ is the quantum dilogarithm in (4.6).

5.1.1. Normalization. Dividing the partition function with two condensates and a single-brane insertion by its counterpart that has no single-brane insertion (4.5), we obtain the normalized partition function,

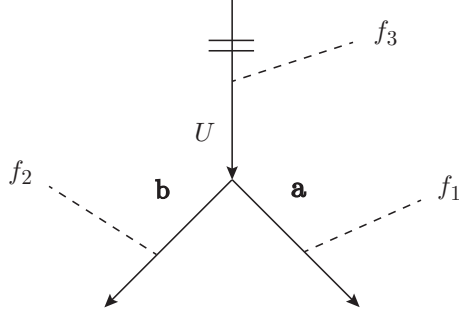


FIGURE 5.1. The partition function with a single-brane insertion that has an open string modulus U and framing factor f_3 , and two infinite stacks of branes that have open string moduli $\mathbf{a} = (a_1, a_2, \dots)$, $\mathbf{b} = (b_1, b_2, \dots)$ and framing factors (f_1, f_2) . By the inverse arrow in the preferred leg we assign the transpose Y'_3 of the Young diagram Y_3 , where we note the relation $\mathcal{R}_{Y_1 Y_2 Y_3}(x, x) = C_{Y_1 Y_2 Y'_3}(x)$ in (3.5).

$$(5.4) \quad Z'_{xy}{}^{(-1,0,f)}(U; \mathbf{a}, \mathbf{b}) = \sum_{d=0}^{\infty} \frac{x^{\frac{1}{2}(1-f)d^2} \left((-1)^{f+1} y^{f/2} U \right)^d}{\prod_{m=1}^d (1-x^m)} \left(\prod_{l=1}^{\infty} \frac{(1-a_l x^{\frac{1}{2}})}{(1-a_l x^{\frac{1}{2}-d})} \prod_{m=1}^d \frac{(1-b_l x^{m-1} y^{-\frac{1}{2}})}{(1-b_l x^{m-1} y^{\frac{1}{2}})} \right)$$

We now show that for a suitable choice of the moduli (a_1, a_2, \dots) and (b_1, b_2, \dots) , the normalized partition function (5.4) of a single-brane insertion and two condensates is the qt -deformation of the partition function on \mathbb{C}^3 with a single-brane insertion (and no condensates). The latter without the qt -deformation is obtained from (5.4) by setting the open string moduli of the condensates to zero,

$$(5.5) \quad Z'_{xy}{}^{(-1,0,f)}(U; 0, 0) = \sum_{d=0}^{\infty} \frac{x^{\frac{1}{2}(1-f)d^2} \left((-1)^{f+1} y^{f/2} U \right)^d}{\prod_{m=1}^d (1-x^m)}$$

5.1.2. *Remark.* By

$$(5.6) \quad s_{(d)}(x^\rho) = x^{\frac{1}{2}d(d-1)} s_{(1^d)}(x^\rho) = \frac{(-1)^d x^{d^2/2}}{\prod_{m=1}^d (1-x^m)},$$

the partition function (5.5) is expressed in terms of the Schur functions as

$$(5.7) \quad \begin{aligned} Z'_{xy}{}^{(-1,0,f)}(U; 0, 0) &= \sum_Y x^{-\frac{1}{2}f d^2} s_Y(x^\rho) s_Y \left((-1)^f y^{\frac{1}{2}f} U \right) \\ &= \sum_Y x^{\frac{1}{2}(1-f)d^2} s_{Y'}(x^\rho) s_Y \left((-1)^f x^{-\frac{1}{2}} y^{\frac{1}{2}f} U \right) \end{aligned}$$

Then, using the Cauchy identities in appendix A, the special cases of (5.5) that correspond to $f = 0, 1$, satisfy,

$$(5.8) \quad Z_{xy}'^{(-1,0,0)}(U; 0, 0) = \left(Z_{xy}'^{(-1,0,1)}(vU; 0, 0) \right)^{-1} = L(U, x)$$

5.2. **The qt -deformation of $Z_{xy}'^{(-1,0,1)}(U; 0, 0)$.** The qt -partition function on \mathbb{C}^3 with a single-brane insertion with an open string modulus U , can be computed using the Macdonald vertex as,

$$(5.9) \quad Z_{xy}^{qt}(U) = \sum_Y \mathcal{M}_{\emptyset \emptyset Y}^{qt}(x, y) s_{Y'}(U) = \sum_{d=0}^{\infty} \left(\prod_{i=0}^{\infty} \prod_{m=1}^d \frac{1 - q^i t x^m}{1 - q^i x^m} \right) U^d$$

By $Z_{xy}'^{(-1,0,1)}(y^{-\frac{1}{2}}U; 0, 0) = Z_{xy}^{qt}(U)$, this qt -partition function can be considered as the qt -deformation of the undeformed partition function (5.5).

5.3. **Identification.** To identify the partition function in (5.4) with that in (5.9), we make the choice of moduli,

$$(5.10) \quad a_l \rightarrow a'_{ij} = x^d a_{ij} = q^i x^{j-\frac{1}{2}+d}, \quad b_l \rightarrow b'_{ij} = x b_{ij} = q^{i-1} t x^{j+\frac{1}{2}}, \quad i, j = 1, 2, \dots$$

instead of that in (4.11). In other words, in this case, the moduli of the brane condensates now depend on the length of the single-row of the Young diagram that labels the Schur function that characterizes the single-brane insertion, d . For this modified choice of moduli, the normalized partition function (5.4) with a single-brane insertion and two condensates becomes,

$$(5.11) \quad Z_{xy}'^{(-1,0,f)}(y^{-\frac{f}{2}}U; a'_{ij}, b'_{ij}) = \sum_{d=0}^{\infty} x^{\frac{1}{2}(1-f)d^2} \left(\prod_{i=0}^{\infty} \prod_{m=1}^d \frac{1 - q^i t x^m}{1 - q^i x^m} \right) \left((-1)^{f+1} U \right)^d,$$

and we find,

$$(5.12) \quad Z_{xy}'^{(-1,0,1)}(y^{-\frac{1}{2}}U; a'_{ij}, b'_{ij}) = \sum_{d=0}^{\infty} \left(\prod_{i=0}^{\infty} \prod_{m=1}^d \frac{1 - q^i t x^m}{1 - q^i x^m} \right) U^d = Z_{xy}^{qt}(U)$$

We conclude that the refined qt -partition function with a single-brane insertion (and no brane condensates) coincides with its undeformed counterpart (with condensates) for a suitable choice of the framing factors, and of the open string moduli of the condensates. Note that this refined qt -partition function does not depend on y , and coincides with the result computed by the original vertex $C_{Y_1 Y_2 Y_3}(x)$ in a similar way.

5.3.1. *Back-reaction.* We attribute the change in the choice of the moduli of the condensates from that in (4.11) to that in (5.10) to back-reaction: due to the single-brane insertion, the moduli of the condensates change.

6. qt -DEFORMATIONS AS GEOMETRIC TRANSITIONS

We discuss the relation of brane condensates and geometric transitions in the context of unrefined objects.

6.1. Brane condensates and geometric transitions. Following Gomis and Okuda [21, 22], brane insertions change the topology of a Calabi-Yau 3-fold *via* a geometric transition [23], and a Calabi-Yau 3-fold with brane insertions is equivalent to a bubbling Calabi-Yau 3-fold of a more complicated topology, but without brane insertions. Correspondingly, an interpretation of the result in section 4.3 is that a brane condensate (which is infinitely-many brane insertions) changes the topology of \mathbb{C}^3 *via* a geometric transition, and \mathbb{C}^3 with brane condensates is equivalent to another Calabi-Yau 3-fold of a more complicated geometry, but without brane condensates. To test this interpretation, we consider the qt -MacMahon generating function M_{xx}^{qt} in (2.9), which, as we showed in section 4.3, is equal to the open string partition on \mathbb{C}^3 with two condensates, and interpret it as an undeformed (no brane condensates) closed string partition function on a Calabi-Yau 3-fold with more complicated topology than \mathbb{C}^3 .

6.2. Gopakumar-Vafa invariants. The partition function $Z_X(x, \mathbf{Q})$ of the string on a Calabi-Yau 3-fold X with (exponentiated) Kähler moduli \mathbf{Q} , is the generating function of Gopakumar-Vafa invariants $n_{\beta, g} \in \mathbb{Z}$ [24],

$$(6.1) \quad Z_X(x, \mathbf{Q}) = \exp \left(\sum_{\beta \in H_2(X, \mathbb{Z})} \sum_{g=0}^{\infty} \sum_{n=1}^{\infty} \frac{n_{\beta, g}}{n} (x^{n/2} - x^{-n/2})^{2g-2} \mathbf{Q}^{\beta n} \right),$$

where we have followed the notation used in [38]. Namely, if $i = (1, 2, \dots, b_2)$, where b_2 is the second Betti number of X , S_i is a basis of the second homology group $H_2(X, \mathbb{Z})$, and Q_i are (exponentiated) Kähler parameters, then for any $\beta = \sum_i n_i [S_i] \in H_2(X, \mathbb{Z})$, $n_i \in \mathbb{Z}$, $\mathbf{Q}^\beta = \prod_i Q_i^{n_i}$. Comparing M_{xx}^{qt} in (2.9) normalized by M_{xx} in (2.7) and the expansion in (6.1), we find that $n_{\beta, 0} = \pm 1$, $n_{\beta, g} = 0$, for $g = 1, 2, \dots$, which are the Gopakumar-Vafa invariants of a genus-0 manifold with infinitely-many homology 2-cycles β . This agrees with our interpretation of the qt -deformation in terms of a geometric transition driven by a brane condensate, that is, the insertion of infinitely-many branes. In section 7, we identify this geometry with that of an infinite strip, but before we do that, we consider a simple, but important example.

6.3. A simple example of a geometric transition. In the special case of $q = 0$, $t \neq 0$, the qt -MacMahon generating function (2.9) is,

$$(6.2) \quad M_{xx}^{0t} = M_{xx} \prod_{m=1}^{\infty} (1 - t x^m)^m$$

This coincides with the undeformed closed string partition function on the resolved conifold, which is the total space of $\mathcal{O}(-1) \oplus \mathcal{O}(-1) \rightarrow \mathbb{P}^1$ with a single (exponentiated) Kähler modulus t , in agreement with the interpretation of the t -deformation of the MacMahon's generating function proposed in [47].⁹ From the perspective of this section, what we have is the simple geometric transition in Fig. 6.1.

⁹ What we call a t -deformation is called a Q -deformation in [47].

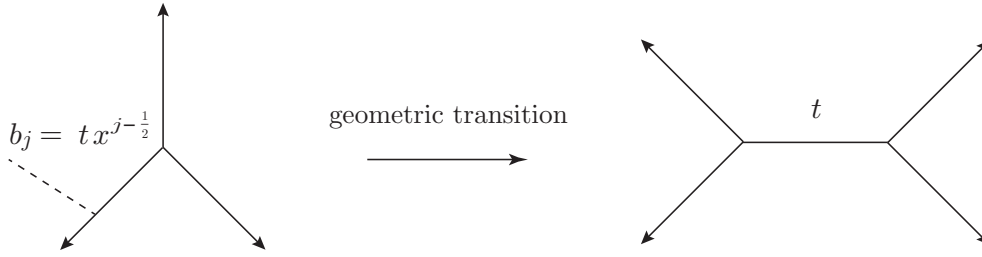


FIGURE 6.1. The figure on the left represents the partition function with a single-brane insertion on \mathbb{C}^3 . The figure on the right represents the closed string partition function on the resolved conifold. They are related by a geometric transition.

7. qt -QUANTUM CURVES

We discuss the qt -quantum curves associated with the unrefined limit of the refined qt -deformed brane partition function in section 5.

7.1. The quantum curve for $Z^{qt}(U)$.

7.1.1. *Two operators.* Consider the operators \widehat{U} and \widehat{V} , where \widehat{U} acts as multiplication by a variable U , and \widehat{V} acts as,

$$(7.1) \quad \widehat{V} := x^{U \frac{d}{dU}}$$

They satisfy the x -Weyl relation,

$$(7.2) \quad \widehat{V} \widehat{U} = x \widehat{U} \widehat{V},$$

and act on $Z^{qt}(U)$, the unrefined limit of the refined qt -deformed brane partition (5.9), as,

$$(7.3) \quad \widehat{U} Z^{qt}(U) = U Z^{qt}(U), \quad \widehat{V} Z^{qt}(U) = Z^{qt}(xU)$$

7.1.2. *The quantum curve.* From (7.3), it follows that $Z^{qt}(U)$ satisfies the x -difference equation,

$$(7.4) \quad \widehat{A}^{qt}(\widehat{U}, \widehat{V}) Z^{qt}(U) := \left(\prod_{i=0}^{\infty} (1 - q^i \widehat{V}) - \widehat{U} \prod_{i=0}^{\infty} (1 - q^i t x \widehat{V}) \right) Z^{qt}(U) = 0,$$

which is the *quantum curve* related to $Z^{qt}(U)$. As discussed below, (7.4) is a qt -version of the quantum curve of \mathbb{C}^3 in string theory [1, 16, 15, 25].

7.1.3. *The classical limit of the quantum curve.* Assuming that the asymptotic expansion of $Z^{qt}(U)$ in the classical limit, $g_s = -\log x \rightarrow 0$, has the form,

$$(7.5) \quad Z^{qt}(U) \sim \exp \left(-\frac{1}{g_s} \int^U \log V(U') \frac{dU'}{U'} \right),$$

then $V(U)$ is a solution of the equation,

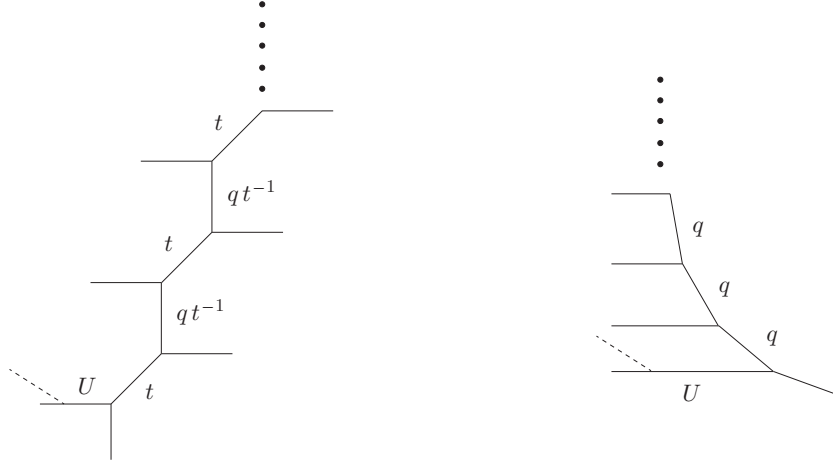


FIGURE 7.1. The figure on the left describes the infinite chain of $(-1, -1)$ curves with Kähler moduli t and qt^{-1} , and a brane insertion with the open string modulus U . The figure on the right describes the infinite chain of $(-2, 0)$ curves with Kähler moduli q , and a brane insertion with the open string modulus U .

$$(7.6) \quad A^{qt} (U, V(U)) := \prod_{i=0}^{\infty} (1 - q^i V(U)) - U \prod_{i=0}^{\infty} (1 - q^i t V(U)) = 0,$$

which is *the classical curve* related to $Z^{qt}(U)$. This curve can be identified with the mirror curve related to the infinite-strip geometry that consists of an infinite chain of $(-1, -1)$ -curves, see the figure on the left in Fig. 7.1 [31] (see also [20]). This infinite-strip geometry agrees with the picture of infinite-stacks of branes, or equivalently brane condensates in sections 4, 5 and 6. In the remainder of this section, we consider a number of special cases of quantum curves.

7.2. Case 1. Choosing $q = t$, the brane partition function (5.9) reduces to the undeformed partition function $Z'_{xx}{}^{(-1,0,1)}(x^{-\frac{1}{2}}U; 0, 0)$ with a single-brane insertion on \mathbb{C}^3 in (5.5),

$$(7.7) \quad Z^{qq}(U) = \sum_{d=0}^{\infty} \frac{1}{\prod_{m=1}^d (1 - x^m)} U^d = Z'_{xx}{}^{(-1,0,1)}(x^{-\frac{1}{2}}U; 0, 0) = L(x^{-\frac{1}{2}}U, x)^{-1},$$

and we find the quantum curve,

$$(7.8) \quad (1 - \widehat{V} - \widehat{U}) Z^{qq}(U) = 0$$

The classical limit, $g_s \rightarrow 0$, of the quantum curve (7.8) gives a mirror curve of \mathbb{C}^3 [3],

$$(7.9) \quad 1 - U - V = 0$$

In other words, the qt -quantum curve (7.4) is a qt -version of the quantum curve (7.8), and (7.6) is a qt -version of the mirror curve (7.9).

7.3. **Case 2.** Choosing $q = 0$ and $t \neq 0$, the brane partition function (5.9) reduces to,

$$(7.10) \quad Z^{0t}(U) = \sum_{d=0}^{\infty} \left(\prod_{m=1}^d \frac{1-tx^m}{1-x^m} \right) U^d,$$

and we find the t -version of the quantum curve of \mathbb{C}^3 ,

$$(7.11) \quad (1 - \widehat{V} - \widehat{U} + t \widehat{V} \widehat{U}) Z^{0t}(U) = 0$$

Note that $Z^{0t}(U)$ agrees with the undeformed brane partition function, up to framing ambiguities, on the resolved conifold with the Kähler modulus t [47], and the classical limit, $g_s \rightarrow 0$, of the quantum curve (7.11) is the mirror curve of the resolved conifold [3],

$$(7.12) \quad 1 - U - V + tUV = 0$$

In other words, the t -deformation of \mathbb{C}^3 is the resolved conifold as discussed in section 6.3.

7.4. **Case 3.** Choosing $q \neq 0$ and $t = 0$, the brane partition function (5.9) reduces to,

$$(7.13) \quad Z^{q0}(U) = \sum_{d=0}^{\infty} \frac{1}{\prod_{i=0}^{\infty} \prod_{m=1}^d (1 - q^i x^m)} U^d,$$

and the q -version of the quantum curve of \mathbb{C}^3 is,

$$(7.14) \quad \left(\prod_{i=0}^{\infty} (1 - q^i \widehat{V}) - \widehat{U} \right) Z^{q0}(U) = 0$$

$Z^{q0}(U)$ agrees with the undeformed brane partition function, up to framing ambiguities and a slight modification of the Kähler moduli, for the infinite chain of $(-2, 0)$ -curves,

$$(7.15) \quad \mathcal{O}(-2) \oplus \mathcal{O}(0) \rightarrow \mathbb{P}^1,$$

with the same Kähler modulus q for all \mathbb{P}^1 , see the figure on the right in Fig. 7.1 [31] (see also [20]). This infinite-strip geometry can be obtained from that in the figure on the left in Fig. 7.1 by suitable blow-downs.¹⁰ The classical limit, $g_s \rightarrow 0$, of the quantum curve (7.14) is the mirror curve of this strip geometry,

$$(7.16) \quad \prod_{i=0}^{\infty} (1 - q^i V) - U = 0$$

We argue that the q -deformation of \mathbb{C}^3 is identified with the infinite-strip geometry in the figure on the right in Fig. 7.1, and that this infinite-strip geometry is the result of a geometric transition caused by the brane condensates.

¹⁰ Starting from the infinite-strip geometry on the left in Fig. 7.1, one can think of what happens in the limit $t \rightarrow 0$ as follows. As $t \rightarrow 0$, the Kähler parameters t vanish, while the Kähler parameters q/t diverge, and the corresponding consecutive edges in the toric diagram combine in pairs to form a toric diagram that has edges with finite Kähler parameters q . The new infinite-strip geometry is on the right in Fig. 7.1.

8. REMARKS

We collect a number of remarks, with particular attention to the interpretation of the various parameters that can appear in topological vertices, and to the relation with conformal field theory.

8.1. The AGT counterpart of brane condensation. We showed that the Macdonald-type qt -deformation introduced in [50], when applied to topological string partition functions [18], leads to qt -partition functions that are equivalent to partition functions without a qt -deformation but with brane condensates. These brane condensates are surface operator condensates, and their counterparts on the conformal field theory side of the AGT correspondence are vertex operator condensates in 2D chiral conformal blocks. While this has not been studied in any detail, we expect that these vertex operator condensates play, at the level of conformal blocks, the same role that switching-on off-critical perturbations plays, at the level of the correlation functions [52], and that results in correlation functions in 2D off-critical integrable models. This expectation coincides with the results in [11, 12, 43, 44, 46].¹¹

8.2. Four parameters. If we start from a 4D instanton partition function in the absence of an Ω -background, or an AGT-equivalent conformal block in a Gaussian 2D conformal field theory with an integral central charge, there are four known ways to modify such a partition function, or conformal block, and each of these ways is characterized by a parameter.

8.2.1. The radius of the M -theory circle, R . Topological string partition functions are 5D objects, and the corresponding instanton partition functions live in $\mathbb{R}^4 \times S^1$, where S^1 is the M -theory circle. For small R , one can think of the 5D instanton partition functions as R -deformations of their 4D limits, in the sense that switching on R gradually is equivalent to including the lighter Kaluza-Klein modes that are infinitely-massive in the $R \rightarrow 0$, and that acquire finite masses as R increases [30]. In 2D conformal field theory terms, switching R on is equivalent to deforming the chiral conformal blocks away from criticality to obtain expectation values of type-I vertex operators [14], in some off-critical integrable statistical mechanical models [11, 12, 43, 44, 46].

8.2.2. The refinement parameter x/y . Starting with 4D instanton partition functions in the absence of an Ω -background, one can switch on Nekrasov's Ω -deformation parameters, that is $\epsilon_1 + \epsilon_2 \neq 0$. In the presence of a finite M -theory circle of radius R , setting $x = e^{-R\epsilon_1}$, and $y = R^{R\epsilon_2}$, this refinement is equivalent to setting $x/y \neq 1$. In 2D conformal field theory terms, we modify the central charge of the conformal field theory while preserving conformal invariance, and the underlying statistical mechanical model remains critical.

8.2.3. The Macdonald deformation parameter q/t . The q/t -deformation of [50, 18] is yet another perturbation but, so far, no interpretation of this deformation is known. The purpose of this work is to offer one such interpretation.

8.2.4. The elliptic nome p . In [53, 19], two versions of a vertex based on Saito's elliptic deformation of the quantum toroidal algebra $U_q \left(\widehat{\mathfrak{gl}}_1 \right)$ are proposed. In addition to the refinement parameters (x, y) , and the Macdonald-type deformation parameters (q, t) , this vertex depends on an elliptic nome parameter p and copies of the $(q = t)$ -limit of this vertex can be glued to obtain elliptic conformal blocks. The latter are equal to the elliptic conformal blocks

¹¹ See further discussion on section 8.2.1.

that were computed in [33, 42] by gluing copies of the refined vertex of [32], then gluing pairs of external legs.

8.3. Three off-critical deformations. Aside from the refinement parameter x/y , which preserves criticality, it appears that we have three parameters that push the underlying 2D conformal blocks off-criticality, namely the M -theory circle radius R , the Macdonald parameter q/t , and the nome parameter p . One can show by explicit computation that these three parameters coexist and that their effects are different, but it remains unclear how to interpret these effects in statistical mechanics terms.

8.4. Summary. In [9, 10, 32], a refinement of the original topological vertex was obtained, and the physical meaning of this refinement was clear and related to switching-on a non-self-dual Ω -background. In [50], an independent Macdonald-type qt -deformation of MacMahon's generating function of plane partitions was obtained, and was used in [18] to qt -deformed the refined topological vertex, but no physical meaning of this deformation was proposed. In this work, we have presented a number of simple but clear examples of qt -deformed topological string partition functions, and showed in sections 4 and 5 that, in these cases, the qt -deformation is equivalent to switching-on infinitely-many brane insertions, or equivalently brane condensates. In section 6, we showed that a Calabi-Yau 3-fold with a simple topology in the presence of these condensates is equivalent to another Calabi-Yau 3-fold with a more complicated topology without condensates, and argued that the condensates cause the Calabi-Yau 3-fold on which the topological string theory is formulated to undergo a geometric transition that changes its topology. Finally, in section 7, we studied the qt -quantum curves related to the unrefined limit of the qt -partition functions studied in section 5, and showed that their classical limit does indeed correspond to undeformed partition functions on infinite-strip geometry, in agreement with the conclusion that the qt -deformation is equivalent to brane condensates that drive a geometric transition. We expect these conclusions to hold for qt -deformations of more complicated topological string partition functions.

APPENDIX A. USEFUL SCHUR FUNCTION IDENTITIES

The skew Schur functions satisfy the identities,

$$(A.1) \quad s_Y(x^\rho) = x^{\frac{1}{2}\kappa_Y} s_{Y'}(x^\rho),$$

$$(A.2) \quad s_Y(x^{-\rho}) = x^{\frac{1}{2}\|Y'\|^2} \prod_{\square \in Y} \frac{1}{1 - x^{H_\square}},$$

$$(A.3) \quad s_{Y/\emptyset}(\mathbf{x}) = s_Y(\mathbf{x}),$$

$$(A.4) \quad s_{Y_1/Y_2}(\mathbf{x}) = 0 \quad \text{for } Y_1 \not\supseteq Y_2,$$

$$(A.5) \quad s_{Y_1/Y_2}(c\mathbf{x}) = c^{|Y_1| - |Y_2|} s_{Y_1/Y_2}(\mathbf{x}), \quad c \in \mathbb{C},$$

$$(A.6) \quad s_{Y_1/Y_2}(x^{\rho+Y}) = (-1)^{|Y_1| - |Y_2|} s_{Y'_1/Y'_2}(x^{-\rho-Y})$$

The Cauchy identities for the skew Schur functions are,

$$(A.7) \quad \sum_Y s_{Y/Y_1}(\mathbf{x}) s_{Y/Y_2}(\mathbf{y}) = \sum_Y s_{Y_2/Y}(\mathbf{x}) s_{Y_1/Y}(\mathbf{y}) \prod_{i,j=1} \left(\frac{1}{1-x_i y_j} \right),$$

$$(A.8) \quad \sum_Y s_{Y/Y_1}(\mathbf{x}) s_{Y'/Y_2}(\mathbf{y}) = \sum_Y s_{Y'_2/Y}(\mathbf{x}) s_{Y'_1/Y'}(\mathbf{y}) \prod_{i,j=1} (1+x_i y_j)$$

ACKNOWLEDGEMENTS

We thank Piotr Sułkowski for useful discussions, and the Mathematical Research Institute MATRIX, in Creswick, Victoria, Australia, for hospitality during the workshop ‘*Integrability in Low-Dimensional Quantum Systems*’, where this work was started. The work of OF is supported by the Australian Research Council Discovery Grant DP140103104. The work of MM was supported by the ERC Starting Grant no. 335739 ‘*Quantum fields and knot homologies*’ funded by the European Research Council under the European Union’s Seventh Framework Programme, and currently by the Max-Planck-Institut für Mathematik in Bonn.

REFERENCES

- [1] M Aganagic, R Dijkgraaf, A Klemm, M Mariño, and C Vafa, *Topological strings and integrable hierarchies*, Communications in Mathematical Physics **261** (2006) 451-516, arXiv:0312085 [hep-th].
- [2] M Aganagic, A Klemm, M Mariño, and C Vafa, *The topological vertex*, Communications in Mathematical Physics **254** (2005) 425-478, arXiv:0305132 [hep-th].
- [3] M Aganagic and C Vafa, *Mirror symmetry, D-branes and counting holomorphic discs*, arXiv:0012041 [hep-th].
- [4] L F Alday, D Gaiotto, S Gukov, Y Tachikawa, and H Verlinde, *Loop and surface operators in $\mathcal{N} = 2$ gauge theory and Liouville modular geometry*, Journal of High Energy Physics **1001** (2010) 113, arXiv:0909.0945 [hep-th].
- [5] L F Alday, D Gaiotto, and Y Tachikawa, *Liouville Correlation Functions from Four-dimensional Gauge Theories*, Letters in Mathematical Physics **91** (2010) 167-197, arXiv:0906.3219 [hep-th].
- [6] L F Alday and Y Tachikawa, *Affine $SL(2)$ conformal blocks from 4d gauge theories*, Letters in Mathematical Physics **94** (2010) 87-114, arXiv:1005.4469 [hep-th].
- [7] H Awata, B Feigin, and J Shiraishi, *Quantum Algebraic Approach to Refined Topological Vertex*, Journal of High Energy Physics **1203** (2012) 041, arXiv:1112.6074 [hep-th].
- [8] H Awata, H Fuji, H Kanno, M Manabe, and Y Yamada, *Localization with a Surface Operator, Irregular Conformal Blocks and Open Topological String*, Advances in Theoretical and Mathematical Physics **16**, no. 3 (2012) 725-804, arXiv:1008.0574 [hep-th].
- [9] H Awata and H Kanno, *Instanton counting, Macdonald functions and the moduli space of D-branes*, Journal of High Energy Physics **0505** (2005) 039, arXiv:0502061 [hep-th].
- [10] H Awata and H Kanno, *Refined BPS state counting from Nekrasov’s formula and Macdonald functions*, International Journal of Modern Physics A **24** (2009) 2253-2306, arXiv:0805.0191 [hep-th].
- [11] H Awata and Y Yamada, *Five-dimensional AGT conjecture and the deformed Virasoro algebra*, Journal of High Energy Physics **1001** (2010) 125, arXiv:0910.4431.
- [12] H Awata and Y Yamada, *Five-dimensional AGT Relation and the Deformed beta-ensemble*, Progress in Theoretical Physics **124** (2010) 227-262, arXiv:1004.5122.

- [13] A Braverman, B Feigin, M Finkelberg, and L Rybnikov, *A Finite analog of the AGT relation I: Finite W -algebras and quasimaps' spaces*, Communications in Mathematical Physics **308** (2011) 457, arXiv:1008.3655 [math.AG].
- [14] B Davies, O Foda, M Jimbo, T Miwa, and A Nakayashiki, *Diagonalization of the XXZ Hamiltonian by vertex operators*, Communications in Mathematical Physics **151.1** (1993) 89-153, arXiv:9204064 [hep-th].
- [15] R Dijkgraaf, L Hollands, and P Sułkowski, *Quantum Curves and D-Modules*, Journal of High Energy Physics **0911** (2009) 047, arXiv:0810.4157 [hep-th].
- [16] R Dijkgraaf, L Hollands, P Sułkowski, and C Vafa, *Supersymmetric gauge theories, intersecting branes and free fermions*, Journal of High Energy Physics **0802** (2008) 106, arXiv:0709.4446 [hep-th].
- [17] T Dimofte, S Gukov, and L Hollands, *Vortex Counting and Lagrangian 3-manifolds*, Letters in Mathematical Physics **98** (2011) 225-287, arXiv:1006.0977 [hep-th].
- [18] O Foda and J F Wu, *A Macdonald refined topological vertex*, Journal of Physics A **50** (2017) 294003, arXiv:1701.08541 [hep-th].
- [19] O Foda, J-F Wu, and R-D Zhu, *in preparation*.
- [20] H Fuji, K Iwaki, M Manabe and I Satake, *Reconstructing GKZ via topological recursion*, arXiv:1708.09365 [math-ph].
- [21] J Gomis and T Okuda, *Wilson loops, geometric transitions and bubbling Calabi-Yau's*, Journal of High Energy Physics **0702** (2007) 083, arXiv:0612190 [hep-th].
- [22] J Gomis and T Okuda, *D-branes as a Bubbling Calabi-Yau*, Journal of High Energy Physics **0707** (2007) 005, arXiv:0704.3080 [hep-th].
- [23] R Gopakumar and C Vafa, *On the gauge theory/geometry correspondence*, Advances in Theoretical and Mathematical Physics **3** (1999) 1415, arXiv:9811131 [hep-th].
- [24] R Gopakumar and C Vafa, *M theory and topological strings. 2.*, arXiv:9812127 [hep-th].
- [25] S Gukov and P Sułkowski, *A-polynomial, B-model, and Quantization*, Journal of High Energy Physics **1202** (2012) 070, arXiv:1108.0002 [hep-th].
- [26] S Gukov and E Witten, *Gauge Theory, Ramification, And The Geometric Langlands Program*, arXiv:0612073 [hep-th].
- [27] N Halmagyi, A Sinkovics, and P Sułkowski, *Knot invariants and Calabi-Yau crystals*, Journal of High Energy Physics **0601** (2006) 040, arXiv:0506230 [hep-th].
- [28] R Harvey and H B Lawson, *Calibrated Geometries*, Acta Mathematica **148** (1982) 47-157.
- [29] T J Hollowood, A Iqbal, and C Vafa, *Matrix models, geometric engineering and elliptic genera*, Journal of High Energy Physics **0803** (2008) 069, arXiv:0310272 [hep-th].
- [30] A Iqbal and V S Kaplunovsky, *Quantum deconstruction of a 5D SYM and its moduli space*, Journal of High Energy Physics **0405** (2004) 013, arXiv:0212098 [hep-th].
- [31] A Iqbal and A K Kashani-Poor, *The Vertex on a strip*, Advances in Theoretical and Mathematical Physics **10**, no. 3 (2006) 317-343, arXiv:0410174 [hep-th].
- [32] A Iqbal, C Kozcaz, and C Vafa, *The Refined topological vertex*, Journal of High Energy Physics **0910** (2009) 069, arXiv:0701156 [hep-th].
- [33] A Iqbal, C Kozcaz, and S-T Yau, *Elliptic Virasoro Conformal Blocks*, arXiv:1511.00458.
- [34] H Kanno and Y Tachikawa, *Instanton counting with a surface operator and the chain-saw quiver*, Journal of High Energy Physics **1106** (2011) 119, arXiv:1105.0357 [hep-th].
- [35] S H Katz, A Klemm, and C Vafa, *Geometric engineering of quantum field theories*, Nuclear Physics B **497** (1997) 173-195, arXiv:9609239 [hep-th].
- [36] S Katz, P Mayr, and C Vafa, *Mirror symmetry and exact solution of 4d $N = 2$ gauge theories I*, Advances in Theoretical and Mathematical Physics **1** (1998) 53-114, arXiv:9706110 [hep-th].

- [37] C Kozcaz, S Pasquetti, and N Wyllard, *A & B model approaches to surface operators and Toda theories*, Journal of High Energy Physics **1008** (2010) 042, arXiv:1004.2025 [hep-th].
- [38] M Mariño, *Chern-Simons theory and topological strings*, Reviews of Modern Physics **77** (2005) 675, arXiv:0406005 [hep-th].
- [39] M Mariño and C Vafa, *Framed knots at large N*, Contemporary Mathematics **310** (2002) 185-204, arXiv:0108064 [hep-th].
- [40] N A Nekrasov, *Seiberg-Witten prepotential from instanton counting*, Advances in Theoretical and Mathematical Physics **7**, no. 5 (2003) 831-864, arXiv:0306211 [hep-th].
- [41] N Nekrasov and A Okounkov, *Seiberg-Witten theory and random partitions*, Progress in Mathematics **244** (2006) 525, arXiv:0306238 [hep-th].
- [42] F Nieri, *An elliptic Virasoro symmetry in 6d*, Letters in mathematical physics **107**, no. 11 (2017) 2147-2187, arXiv:1511.00574.
- [43] F Nieri, S Pasquetti, and F Passerini, *3d & 5d gauge theory partition functions as q-deformed CFT correlators*, Letters in Mathematical Physics **105**, no. 1 (2015) 109-148, arXiv:1303.2626 [hep-th].
- [44] F Nieri, S Pasquetti, F Passerini, and A Torrielli, *5D partition functions, q-Virasoro systems and integrable spin-chains*, Journal of High Energy Physics **1412** (2014) 40, arXiv:1312.1294 [hep-th].
- [45] A Okounkov, N Reshetikhin, and C Vafa, *Quantum Calabi-Yau and classical crystals*, Progress in Mathematics **244** (2006) 597, arXiv:0309208 [hep-th].
- [46] S Pasquetti, *Holomorphic blocks and the 5d AGT correspondence*, Journal of Physics A **50**, no. 44 (2017) 443016, arXiv:1608.02968 [hep-th].
- [47] P Sułkowski, *Deformed boson-fermion correspondence, Q-bosons, and topological strings on the conifold*, Journal of High Energy Physics **0810** (2008) 104, arXiv:0808.2327 [hep-th].
- [48] M Taki, *Refined Topological Vertex and Instanton Counting*, Journal of High Energy Physics **0803** (2008) 048, arXiv:0710.1776 [hep-th].
- [49] M Taki, *Surface Operator, Bubbling Calabi-Yau and AGT Relation*, Journal of High Energy Physics **1107** (2011) 047, arXiv:1007.2524 [hep-th].
- [50] M Vuletić, *A generalization of MacMahon's formula*, Transactions of the American Mathematical Society **361** (2009) 2789-2804, arXiv:0707.0532 [math.CO].
- [51] N Wyllard, *A_{N-1} conformal Toda field theory correlation functions from conformal $\mathcal{N} = 2$ $SU(N)$ quiver gauge theories*, Journal of High Energy Physics **0911** (2009) 002, arXiv:0907.2189 [hep-th].
- [52] A B Zamolodchikov, *Integrals of motion in scaling 3-state Potts model field theory*, International Journal of Modern Physics A **3.03** (1988) 743-750.
- [53] R-D Zhu, *An elliptic vertex of Awata-Feigin-Shiraishi-type for M-strings*, arXiv:1712.10255 [hep-th].

¹ MATHEMATICS AND STATISTICS, UNIVERSITY OF MELBOURNE, ROYAL PARADE, PARKVILLE, VIC 3010, AUSTRALIA

E-mail address: omar.foda@unimelb.edu.au

² MAX-PLANCK-INSTITUT FÜR MATHEMATIK, VIVATSGASSE 7, 53111 BONN, GERMANY

E-mail address: masahidemanabe@gmail.com